npj | sustainable mobility and transport

Article

https://doi.org/10.1038/s44333-026-00109-0

The impact of temperature on battery electric vehicle penetration

Gaia Cervini ✉, Lavan Teja Burra, Jinha Jung & Konstantina Gkritza

Battery electric vehicles (BEVs) experience significant performance declines under suboptimal ambient temperatures, with both heat and cold reducing range, slowing acceleration, and prolonging charging times. These issues may deter adoption, especially in regions with high temperature variability or frequent cold spells. Using a two-way spatial autoregressive fixed effects model and ZIP code-level panel data across 12 US states (2021-2023), we assess how temperature impacts BEV penetration. We find a nonlinear relationship: BEV penetration increases in thermally stable areas but declines once temperature variability exceeds 7.6 °C. Cold exposure also matters: every additional 100 days below 5 °C annually reduces BEV share by 0.25%. These results position temperature as a key factor shaping BEV penetration in the US, underscoring the importance of targeted policy measures and technological advancements to enhance vehicle performance and consumer confidence across a broader range of climatic conditions.

Battery electric vehicles (BEVs) have gained momentum in the United States (US), driven by expanding charging infrastructure and sustained policy support. Nationally, BEV sales rose from 1.6% of new light-duty vehicles in 2020 to 9.5% by early 2025[1]. Yet BEV market penetration remains highly uneven across regions. In 2023, California alone accounted for over 1.25 million BEV registrations—more than one-third of the national total—followed by Texas and Florida with over 200,000 vehicles each[2]. In contrast, many states in the Midwest and South recorded BEV counts in the low five digits. These stark regional differences suggest that infrastructure availability, economic conditions, and policy incentives, while important, are not the only factors shaping BEV diffusion in the US.

One plausible factor that may explain this spatial heterogeneity in BEV penetration is ambient temperature. Lithium-ion batteries, the core component of BEVs, exhibit strong sensitivity to thermal conditions. In cold weather, the electrochemical efficiency of battery cells declines, resulting in a driving range loss of up to 41% at approximately -6 °C, compared to only a 10% decrease for internal combustion engine vehicles (ICEVs)[3–9]. Cold temperatures also slow vehicle acceleration, reduce regenerative breaking capability, and can double charging times at -10 °C, forcing BEV drivers to contend with longer charging queues and extended wait times[9–13]. Moreover, the additional energy demand required for heating, ventilation, and air conditioning of the cabin places further strain on the battery, exacerbating these effects[3,4,12–14]. At the other end of the thermal spectrum, elevated temperatures may degrade BEV batteries and shorten their lifespan, thereby elevating overall ownership costs and lifetime carbon footprints[15]. High heat also increases the likelihood of battery overheating, potentially triggering thermal runaway and lead to a BEV fire[12,13,16].

The temperature sensitivity of BEVs can pose substantial challenges not only to private BEV penetration, but also to the electrification of freight transport and public transit. BEVs experience greater efficiency losses than ICEVs on trips exceeding 200 km, especially when traversing regions with large temperature variations[17]. This can be of particular concern for long-haul trucking fleets that operate across vast and varied climatic zones. As for public transit, battery-electric buses can consume up to 48% more energy in cold weather, driven by cabin heating, ventilation, and air conditioning (HVAC) demands, reduced regenerative braking efficiency, high energy use during idling, and battery preheating[18].

These performance constraints not only challenge the operational viability of BEVs, but also contribute to consumers' skepticism regarding BEV reliability[19], potentially slowing adoption in multiple key sectors. Consumer surveys in China show that concerns about vehicle performance—including battery life, charging time, and durability—rank among the top deterrents for prospective BEV users[20]. Broader international survey evidence also suggests that performance-related concerns—including range limitations, large battery size, and general uncertainty about BEV reliability—consistently reduce adoption intent across diverse markets[21–23]. In regions with extreme temperatures, skepticism regarding battery durability and safety has emerged as a notable barrier to adoption. Alotaibi et al.[24] emphasized that in oil-producing nations with hot climates, the perception of battery safety and degradation under heat can hinder the uptake of BEV technology.

In view of the above, this study investigates whether ambient temperature contributes to regional disparities in BEV penetration across the US. We hypothesize that locations characterized by greater temperature

Lyles School of Civil and Construction Engineering, Purdue University, West Lafayette, IN, US. ✉e-mail: gcervini@purdue.edu

seasonality and frequent cold weather are associated with lower BEV penetration, given the well-documented sensitivity of battery performance to thermal extremes. Furthermore, we anticipate a nonlinear relationship, as the negative effects of temperature on BEV performance tend to intensify beyond specific thermal thresholds.

Literature Review

Although the impacts of temperature on BEV performance are well documented, their broader implications for consumer adoption remain understudied. Most existing research tends to focus on the impact of financial incentives, infrastructure, and sociodemographic-related factors[25–33], overlooking how climate conditions may shape demand. Yet, consumer demand in many markets—including food, beverages, tourism, apparel, and retail—is known to be sensitive to climatic variability[34], suggesting that vehicle preferences may also be climate-contingent.

So far, emerging international evidence supports this view. In China, provinces characterized by moderate temperatures exhibited higher BEV sales in 2018 than provinces characterized by more extreme temperatures[34]. Of the provinces characterized by more extreme temperatures, those that were cold exhibited lower sales than those that were hot, indicating that cold temperatures exert a stronger deterrent effect on BEV adoption[34]. A similar pattern has been observed in Norway in 2020, where colder municipalities exhibited lower BEV counts[30]. Recent findings from China also show that cold waves between 2016 and 2022 decreased EV sales by 10.1% with each additional occurrence[35].

In the US, however, the relationship between temperature and BEV penetration remains comparatively underexplored and inconclusive. A decade ago, Vergis and Chen[36] observed that colder US regions exhibited lower BEV and plug-in hybrid (PHEV) adoption rates, with BEVs showing greater sensitivity to extreme temperatures likely due to their exclusive reliance on battery power. However, more recent research by Lee et al.[37] found no significant relationship between temperature and zero-emission vehicle adoption at the state level, highlighting the lack of consensus on the issue.

While part of this discrepancy may arise from differences in methodological approaches or the stage of market development captured by each study, a more fundamental issue lies in their use of large geographic units of analysis, which introduces well-known limitations associated with the Modifiable Areal Unit Problem (MAUP): aggregating data to larger spatial units can smooth out local variability and result in loss or distortion of heterogeneity in the data[38]. The MAUP can be particularly problematic when studying the effects of temperature on BEV penetration, as regional (or even state-level) aggregations collapse distinct local climates into a single average. Additionally, such coarse units provide relatively few observations, limiting both statistical power and diminishing the ability to detect geographically nuanced effects of temperature on consumer behavior.

A recent study by Cervini et al.[39] addressed some of these limitations by using ZIP code-level data and found that temperature variability was among the strongest predictors of both BEV and PHEV market penetration and population change rate in the US. However, the machine learning approach adopted, while powerful for prediction, precluded causal inference and did not allow to estimate the direction or magnitude of temperature effects. That study also did not analyze spatial interdependence in BEV penetration, which is a documented phenomenon in transportation behavior[29,30,37].

Overall, existing research does not conclusively establish the extent to which temperature impacts BEV penetration rates across the US and the corresponding spatial heterogeneity. To address this gap, we investigate how local thermal dynamics—including daily temperature variability and cold exposure—shape regional patterns of BEV market share using panel data at the ZIP code level across 12 states spanning a broad range of climate zones.

Our study offers several methodological improvements over previous work. First, we use highly granular spatial units to minimize bias introduced by the MAUP. Second, our dataset is substantially broader than prior studies, covering a wide range of thermal conditions across 12 climatically diverse US states. Third, we introduce novel temperature metrics that capture both intra-annual variability and the frequency of cold weather, enabling a more precise evaluation of temperature influences on penetration. Fourth, we employ econometric models that control for potential confounding variables, allowing us to isolate the effects of temperature on penetration. Finally, we examine spatial autocorrelation and spillover effects, which are often overlooked but they are essential for understanding regional dynamics. Together, these innovations enable a more robust assessment of how local temperature conditions shape BEV uptake in the US, offering actionable insights for policymakers and infrastructure planners seeking to advance transportation electrification.

Results

Temperature Effects

To assess how variation in local temperature impacts BEV penetration, we estimate three spatial panel models of increasing complexity (see Table 1). We start with a baseline fixed effects (FE) specification that includes our key variables of interest—temperature variability and exposure to cold temperatures—along with a rich set of controls capturing access to public charging infrastructure, as well as socioeconomic and built environment factors. Our preferred specification (Model 3 in Table 1) includes a spline-transformed term for daily average temperature variability ($\overline{T}_{iqr}$). This metric captures the typical intra-annual thermal variation experienced in a location; higher values indicate greater seasonal fluctuation in daily temperatures. Incorporating $\overline{T}_{iqr}$ as a nonlinear spline term allows us to flexibly estimate how different levels of temperature variability affect BEV adoption. The model also includes spatial lag and error terms to account for geographic spillovers.

We find robust evidence that temperature dynamics play a significant and nonlinear role in shaping BEV penetration across the US. The estimated partial effect function $f(\overline{T}_{iqr})$ in Fig. 1 indicates that areas characterized by low $\overline{T}_{iqr}$ are associated with up to a 0.72% increase in BEV share. These are locations such as San Diego (CA), for instance, where most daily temperatures hover around 18-24 °C year-round. These mild and stable conditions align closely with the optimal operating temperature range of BEV batteries, potentially explaining the high penetration rates observed in such locations.

However, the positive relationship between temperature and BEV penetration reverses quickly as thermal variability increases. The partial effect curve crosses zero at 7.6 °C, beyond which the estimated change in BEV penetration becomes negative. BEV share decreases by roughly -0.60% at 11.4 °C (15th percentile), by -0.75% at 18.4 °C (85th percentile), and by nearly -0.90% at the highest observed levels of thermal variability. This suggests that ZIP codes with more unstable thermal regimes tend to exhibit significantly lower BEV penetration. Areas with higher $\overline{T}_{iqr}$ value imply greater seasonal or synoptic temperature swings, typical of interior continental climates. For example, spring and fall in Minneapolis (MN) can exhibit swings from below freezing to above 20 °C within weeks. Annual temperature ranges may stretch from -20 °C to 30 °C, with common daily winter means around -10 °C and summer means around 25 °C. The nonlinearity in the partial effect thus implies a threshold beyond which consumers no longer find BEVs attractive, which is reflected in a negative effect on aggregate BEV penetration rates. Figure S1 in Supplementary Information maps the partial effect of $\overline{T}_{iqr}$ for selected states.

Cold extremes independently suppress penetration. Each additional 100 days per year with minimum temperatures below 5 °C ($T_{MIN<5}$) leads to a 0.25% reduction in BEV share, a statistically significant effect that accumulates meaningfully in colder climates. These findings align with empirical studies showing that battery efficiency, cabin heating demands, and overall driving experience deteriorate in sub-freezing conditions, reinforcing user hesitation to transition away from ICEVs in such regions. Range anxiety is also higher during cold months, negatively impacting customer confidence in BEVs. Indeed, both qualitative and quantitative studies have shown that BEV drivers report heightened range anxiety in winter specifically due to the compound effects of battery inefficiency and cabin heating load[40,41].

Table 1 | Regression results for different model specifications

	Model 1	Model 2	Model 3
Estimator	FE OLS	FE SARAR	
No. Observations	25314	25314	25314
R^2	0.6236	0.6587	0.6618
Jarque-Bera test	***	***	***
Modified Wald test	***	***	***
const	1.2788***	-	-
	(0.0835)		
$\overline{T}_{iqr}$	-0.1132***	-0.0516***	-
	(0.0038)	(0.0031)	
$B_1(\overline{T}_{iqr})$	-	-	0.7205***
			(0.0669)
$B_2(\overline{T}_{iqr})$	-	-	-1.3420***
			(0.0608)
$B_3(\overline{T}_{iqr})$	-	-	-1.4783***
			(0.0647)
$B_4(\overline{T}_{iqr})$	-	-	-1.5891***
			(0.1465)
$T_{MIN<5}$	-0.0040***	-0.0026***	-0.0025***
	(0.0002)	(0.0002)	(0.0002)
Station Proximity	0.0889**	0.2689***	0.1699***
	(0.0423)	(0.0332)	(0.0366)
Level 2 Stations	0.1133***	0.1231***	0.1195***
	(0.0206)	(0.0056)	(0.0056)
DCFC Stations	0.8427**	0.7021***	0.6178***
	(0.3700)	(0.0846)	(0.0845)
Housing Density	-0.1671***	-0.1941***	-0.1933***
	(0.0169)	(0.0063)	(0.0063)
Multivehicle HH	-0.0069***	-0.0063***	-0.0081***
	(0.0010)	(0.0006)	(0.0006)
Solar Energy HH	0.0334***	0.0305***	0.0461***
	(0.0107)	(0.0086)	(0.0087)
Public Transit	0.0183***	0.0232***	0.0226***
	(0.0035)	(0.0015)	(0.0015)
Commute Time	-0.0322**	-0.0010	-0.0065
	(0.0142)	(0.0106)	(0.0111)
Income	0.4217***	0.4294***	0.4264***
	(0.0181)	(0.0071)	(0.0071)
Education	0.0415***	0.0453***	0.0452***
	(0.0027)	(0.0013)	(0.0013)
ρ	-	0.1444***	0.1181***
		(0.0102)	(0.0108)
λ	-	0.1226***	0.1260***
		(0.0146)	(0.0149)

Standard errors reported in parentheses.
Significance levels: * $p \leq 0.1$, ** $p < 0.05$, *** $p < 0.01$.

Model comparison in Table 1 confirms the importance of both spatial effects and nonlinear temperature terms. Model 1, a pooled ordinary least squares (OLS) specification with FE, yields a baseline R^2 of 0.624 and omits spatial structure. Adding spatial lag and spatial error terms in Model 2 improves model fit (R^2 = 0.659), while Model 3—which additionally includes $\overline{T}_{iqr}$ piecewise-linear splines—offers the best overall explanatory power (R^2 = 0.662). Model 3 thus provides our preferred specification, capturing both spatial autocorrelation and the complex, threshold-based relationship between thermal variability and BEV penetration. Importantly, we find no evidence that these climatic effects are merely proxies for infrastructure or socioeconomic conditions. Even after controlling for charging infrastructure, income, education, and urbanization, temperature variability and cold exposure retain strong independent explanatory power.

Covariate Effects

While temperature emerges as a strong constraint to BEV penetration, infrastructure access offers the clearest countermeasure. Higher densities of public charging stations—especially DC fast chargers (DCFC)—are consistently associated with greater BEV penetration. In our preferred specification, each additional DCFC per km^2 corresponds to a 0.62% increase in BEV share—more than five times the impact of Level 2 chargers—underscoring the superior role of fast charging in boosting consumers' appeal to BEVs. Importantly, station proximity—not just density—also has a significant and independent effect on BEV penetration, suggesting that convenient, accessible charging is essential to drive consumer uptake. This underscores the role of infrastructure not only in enabling practical charging, but possibly also in reducing the psychological barriers posed by temperature-induced range anxiety.

Other contextual factors further shape the penetration landscape. While BEV uptake declines with increasing housing density—a pattern suggestive of charging limitations—a $10,000 increase in median income is associated with a 0.43% local increase in BEV penetration, underlining the strong influence of wealth on BEV access. Educational attainment also contributes, with each 1% increase in the share of graduate degree holders linked to a 0.045% increase. This may reflect greater tech-savviness, environmental values, or peer influence in higher-education communities. ZIP codes with higher shares of public transit users also exhibit higher BEV penetration, potentially reflecting urban clustering, environmental consciousness, or a preference for using BEVs for short personal trips rather than commuting.

Commute time exhibits a consistent negative relationship with BEV penetration across all models: ZIP codes with longer average travel times to work tend to have lower BEV adoption. However, the explanatory power of commute time diminishes in spatial models, suggesting that its effect may be partly absorbed by spatial spillovers or regional thermal effects.

Finally, we find that the prevalence of residential solar heating is positively associated with BEV penetration. Specifically, a 1% increase in the share of homes using solar panels for heating is associated with a 0.046% increase in BEV penetration. This finding aligns with recent evidence from Hardaway et al.[42], who similarly report that households investing in solar energy are significantly more likely to adopt EVs. This relationship likely reflects the economic and practical advantages of pairing solar energy with EV ownership: households that can generate their own electricity can significantly reduce or eliminate the fuel expenses associated with driving a BEV. As a result, for these households, BEVs offer a clear cost advantage over ICEVs, which remain dependent on purchased gasoline or diesel. The finding may also indicate a broader pattern of environmentally conscious behavior, where penetration of one clean technology (e.g., solar panels) correlates with openness to another (e.g., BEVs).

Spatial Spillovers

The spatial diffusion of BEVs reflects more than localized decision-making; it is embedded in a broader regional context. Model 3 in Table 1 reveals robust spatial effects in BEV penetration across ZIP codes. The spatial autoregressive (or lag) coefficient (ρ = 0.12, $p < 0.01$) confirms that BEV penetration in one area is positively shaped by uptake in adjacent areas, reflecting mechanisms such as peer influence, infrastructure sharing, and regional policy spillovers. In parallel, the spatial error coefficient (λ = 0.13, $p < 0.01$) points to latent (or unobserved) regional factors—such as social norms or consumer preferences—that further entangle BEV trajectories across space.

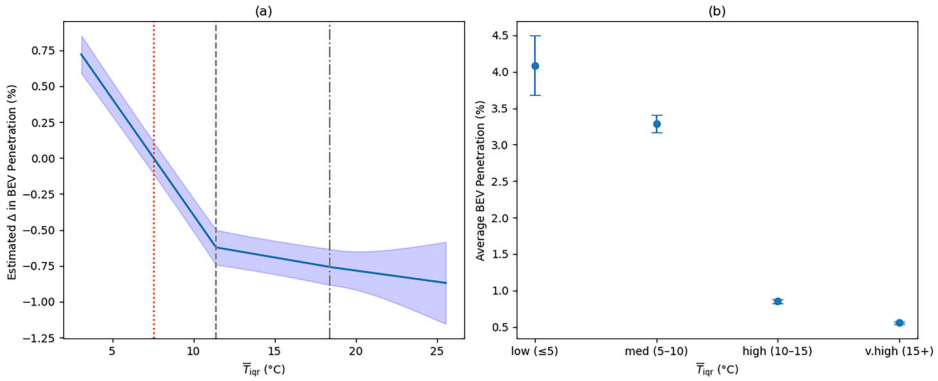

Fig. 1 | Relationship between temperature variability ($\overline{T}_{iqr}$) and BEV penetration. **(a)** shows the estimated partial effect function, $f(x)$, relating $\overline{T}_{iqr}$ to BEV penetration. The solid blue line represents the point estimate of $f(x)$, and the light-blue shaded band indicates the 95% confidence interval. Vertical black dashed lines mark the 15th and 85th percentiles of $\overline{T}_{iqr}$ (11.4 °C and 18.4 °C, respectively). The vertical red dotted line marks the value of $\overline{T}_{iqr}$ (7.6 °C) at which the estimated partial effect crosses zero. **(b)** reports average BEV penetration within four $\overline{T}_{iqr}$ bins: low ≤5 °C, medium 5–10 °C, high 10–15 °C, and very high ≥15 °C.

Table 2 | Direct, indirect, and total effects

Variable	Direct Effect	Indirect Effect	Total Effect
$\overline{T}_{iqr} \leq 11.4℃$	-0.1622	-0.0211	-0.1832
$11.4℃<\overline{T}_{iqr} \leq 18.4℃$	-0.0195	-0.0025	-0.0221
$\overline{T}_{iqr}>18.4℃$	-0.0155	-0.0020	-0.0176
$T_{MIN<5}$	-0.0025	-0.0003	-0.0028
Station Proximity	0.1704	0.0221	0.1925
Level 2 Stations	0.1198	0.0156	0.1354
DCFC Stations	0.6196	0.0805	0.7001
Housing Density	-0.1939	-0.0252	-0.2191
Multivehicle HH	-0.0081	-0.0011	-0.0092
Solar Energy HH	0.0462	0.0060	0.0522
Public Transit	0.0226	0.0029	0.0256
Commute Time	-0.0066	-0.0009	-0.0074
Income	0.4277	0.0556	0.4833
Education	0.0453	0.0059	0.0512

Table 2 summarizes the direct, indirect, and total spatial effects of the independent variables. Importantly, we find that temperature exerts a spatially diffuse influence on BEV penetration: $\overline{T}_{iqr}$ has both nonlinear and regionally contagious effects. At low levels of variability ($\overline{T}_{iqr} \leq 11.4°C$), a one-degree increase in $\overline{T}_{iqr}$ reduces BEV share within a ZIP code by about 0.16% and lowers penetration in neighboring ZIP codes by an additional 0.02%, for a total effect of roughly 0.18%. At moderate and high variability ($11.4°C < \overline{T}_{iqr} \leq 18.4°C$ and $\overline{T}_{iqr} > 18.4°C$), both the direct and indirect effects become smaller in magnitude, with indirect effects on neighbors falling to around 0.002%. In other words, the cost of more unstable temperatures is much larger in places that start out more stable ($\overline{T}_{iqr} \approx 11°C$) and diminishes as baseline variability grows ($\overline{T}_{iqr} \approx 18°C$). These spatial spillovers are statistically detectable but economically modest in magnitude. Overall, however, the results indicate that climate unpredictability imposes not only local constraints on BEV penetration, but also suppresses diffusion in nearby communities, potentially through shared perceptions of technology suitability or regional barriers to charging reliability and performance.

Other variables reinforce the systemic importance of spatial spillovers. The density of DCFC infrastructure in one ZIP code increases BEV penetration in adjacent areas by 0.08%, amplifying its overall effect to 0.7%. This highlights the dual role of DCFC infrastructure—facilitating fast, practical charging for individual users while simultaneously reinforcing regional perceptions of BEV viability and accessibility. Level 2 charging stations, while offering slower charge rates, also exhibit indirect effects of 0.016%. Their broader availability likely supports routine, destination-based charging (e.g., at workplaces or shopping centers), contributing to penetration both within and beyond individual ZIP codes. Although their indirect effect is smaller than that of DCFC, the spatial diffusion suggests that even moderate charging infrastructure can reinforce positive norms and penetration patterns across regions. Proximity to charging infrastructure adds an additional dimension to this dynamic. Beyond the density of stations, the proximity to the nearest public charger yields an indirect effect of 0.022%. This suggests that convenience and visibility of access are central to penetration, not just for individual decision-makers, but for surrounding communities as well. Strategically located charging infrastructure likely reduces range anxiety, normalizes BEV usage, and enhances the perceived reliability of the charging network.

Socioeconomic characteristics also radiate outward: a $10,000 increase in median income yields a 0.05% indirect boost in surrounding areas, while a 1% rise in solar-heated homes and graduate degree attainment correspond to indirect effects of 0.006%. In contrast, densely populated housing areas exhibit negative spillovers (-0.025%), reflecting broader spatial resistance to BEV integration in urbanized settings.

Together, these results emphasize that strategically distributed infrastructure—especially fast chargers and well-placed public stations—can accelerate BEV uptake through both direct accessibility and regional influence. Investments in public charging should thus be guided not only by population or demand densities, but also by spatial considerations that maximize spillover effects across urban and suburban clusters.

Robustness Check

To assess the robustness of our main findings, we conducted a series of model replications across two dimensions: the operationalization of temperature variability and the specification of spatial relationships.

First, we replaced our primary temperature variability measure ($\overline{T}_{iqr}$) with three alternative non-collinear metrics: (1) the standard deviation (σ) of daily minimum temperatures (T_{MIN_σ}), (2) the IQR of daily minimum temperatures ($T_{MIN_{iqr}}$), and (3) the standard deviation of daily mean temperatures ($\overline{T}_\sigma$). These variables were chosen to evaluate whether our conclusions were sensitive to how temperature variation is operationalized (e.g., extremes vs. variability, minimum vs. mean temperatures). Each model maintained the same structure as in Eq. (4), and we evaluated model performance based on changes in coefficient estimates, statistical significance, model fit (R^2), and the Akaike Information Criterion (AIC).

The results, presented in Table S1 in Supplementary Information, confirm the stability of our main findings. All four models, each featuring a different operationalization of temperature, yield consistent direction and significance of key coefficients. Specifically, when using alternative measures such as T_{MIN_σ}, $T_{MIN_{iqr}}$, and $\overline{T}_\sigma$ in place of $\overline{T}_{iqr}$, the relationship between temperature variability and BEV penetration remains negative and statistically significant across all specifications. The coefficient on $\overline{T}_\sigma$ is -0.0738 ($p < 0.001$), on $T_{MIN_{iqr}}$ is -0.0506 ($p < 0.001$), and on T_{MIN_σ} is -0.0686

($p < 0.001$), supporting the conclusion that higher variability in cold or average temperatures suppresses BEV penetration. The other covariates maintain consistent signs and magnitudes across all models. The spatial lag (ρ) and error (λ) parameters also remain statistically significant and stable, confirming that both endogenous interaction effects and unobserved spatial structure are robust features of the BEV penetration process.

Second, we evaluated robustness to spatial weights specification. While our main model uses a Queen contiguity matrix to define spatial dependencies across ZIP codes, we replicated the SARAR model using two additional weighting schemes: (1) a Rook contiguity matrix and (2) an k-nearest-neighbors (KNN) matrix, with k=8. As shown in Supplementary Information Table S2, all coefficients remain directionally and statistically stable across all three spatial configurations. The spatial lag (ρ) and error (λ) terms also remain significant, reinforcing the presence of both endogenous spillovers and unobserved spatial heterogeneity in BEV adoption.

Overall, model fit remains consistent across all specifications ($R^2 \approx 0.66$), with AIC scores differing only slightly, indicating that the models are comparably well-specified. These results provide evidence that our main conclusions are not dependent on a particular choice of temperature variability metric or spatial interaction structure. Additional model comparisons are included in Table S3 in Supplementary Information.

Discussion

This study provides robust empirical evidence that temperature significantly shapes spatial BEV penetration patterns in the US. By leveraging a ZIP code-level panel dataset spanning 12 climatically diverse states from 2021 to 2023 and applying a two-way FE SAREM model, we isolate and quantify the environmental, infrastructural, and sociodemographic determinants of BEV penetration at high spatial resolution.

Our results show that both temperature variability ($\overline{T}_{iqr}$) and frequency of cold weather ($T_{MIN<5}$) have strong, statistically significant negative effects on BEV penetration. These effects are nonlinear, increasing in locations characterized by higher temperature variability. Together, these findings not only underscore the critical influence of environmental conditions on BEV demand, but also reveal a consequential implication for consumers: in regions with colder or hotter climates, BEV ownership may entail substantially higher operating costs due to increased energy consumption driven by thermal stress on batteries. Prior work confirmed that BEV electricity use in the Upper Midwest or Southwest was significantly higher than along the Pacific Coast solely because of ambient temperature differences[4]. Extreme temperatures reduce battery efficiency and increase the frequency and duration of charging events, thereby raising both the financial and temporal burden of ownership. Moreover, in areas where electricity is still heavily reliant on fossil fuels, this elevated energy demand not only inflates consumer costs but also erodes the environmental benefits of BEV penetration. Thus, ambient temperature introduces a geographic inequity in the cost-effectiveness and carbon savings of electrification.

To address the geographic disparities in BEV penetration introduced by temperature, both technological innovation and climate-responsive policy interventions are essential. Automakers should prioritize advancements in battery thermal management systems and vehicle efficiency under varied temperatures. Simultaneously, policymakers should account for local climate realities when crafting incentives and deploying infrastructure. Although this study does not provide a full cost-benefit analysis, our results highlight the types of interventions most likely to relax temperature-related barriers. In particular, we find that public charging infrastructure, especially DCFC, has large direct and spatial spillover effects on BEV penetration, and prior work shows that fast charging is especially effective at reducing range anxiety in cold conditions[43]. Thus, in colder regions where range loss and more frequent charging raise range anxiety and cost of ownership, improving access to fast, reliable public charging is a promising lever for accelerating the transition to electric mobility. Infrastructure investments could also include road electrification technologies, such as dynamic wireless power transfer (DWPT), which could help buffer temperature-related performance drops by reducing the reliance on large battery reserves, especially along major freight or transit corridors[44]. A full economic evaluation of targeted subsidies, DCFC deployment, and complementary technologies, such as DWPT, remains an important direction for future research.

Sociodemographic variables, such as income, education, solar heating, and public transit usage also show consistent positive effects, reinforcing the interplay between clean energy behaviors and BEV diffusion. We also find significant spatial interdependence in BEV penetration, where uptake in one ZIP code boosts penetration in neighboring ZIP codes, even after controlling for local characteristics. The spatial spillovers observed in BEV diffusion underscore the importance of coordinated regional planning. By aligning infrastructure investments across neighboring jurisdictions and leveraging peer effects, policymakers can magnify the impact of local interventions through shared networks and collective momentum. Overall, continued interdisciplinary research on the interaction between climate, technology, and consumer behavior will be key to guiding effective, regionally tailored decarbonization strategies.

This study has several limitations. First, high-resolution public data on BEV registrations remains limited in the US. Our analysis was restricted to ZIP code-level data from just 12 of the 50 states, which constrains geographic coverage and reduces the diversity of BEV penetration contexts represented in the sample. As a result, the findings may not fully capture the heterogeneity of BEV penetration patterns across the broader US landscape. Furthermore, because BEV diffusion remains in its early stages in many states, current data may not yet reflect the long-term dynamics of consumer behavior. Second, the temporal scope of the data was similarly limited. In most states, historical coverage extends back only three to five years, which restricts the ability to evaluate long-term dynamics or policy effects that may evolve over a longer horizon. Third, while we assigned weather station data to ZIP codes using a nearest neighbor approach for spatial matching, more sophisticated interpolation techniques could provide a smoother and potentially more accurate characterization of local climate variability. To assess the potential for interpolation error, we calculated the distances between ZIP code centroids and their assigned weather stations. We find that the median distance between a ZIP code and its nearest station is 10.9 km, with over 94% of ZIP codes falling within 30 km and only 2.9% exceeding 40 km (see Figure S2 in Supplementary Information). While these results suggest that the magnitude of interpolation error is likely limited, the nearest-neighbor method nonetheless introduces an approximation error that should be acknowledged as a limitation of the analysis.

Looking ahead, the strength and shape of the relationships we document in this study are likely to evolve with advances in battery chemistries and thermal management systems. Our estimates are based on a period in which much of the BEV fleet relies on earlier-generation battery packs and thermal management systems, which are more susceptible to performance losses under temperature extremes than the most recent designs. As next-generation vehicles adopt more robust thermal control, higher-efficiency powertrains, and chemistries that are less sensitive to cold and heat, the marginal effect of temperature variability on usable range and charging performance should diminish. In empirical terms, we would expect the negative coefficients on temperature variability and cold-day frequency to attenuate over time, with BEV penetration becoming more tightly linked to charging access, income, and other structural factors. At the same time, perceptions may adjust more slowly than technology: early negative experiences with winter range or cold-weather performance can diffuse through word-of-mouth and social networks, reinforcing skepticism about BEVs even after technical improvements have reduced temperature sensitivity. Because information and reputation spill over across communities, such "perceptual hysteresis" may prolong the impact of climate-related constraints, particularly in regions that have already formed strong narratives about BEVs performing poorly in extreme temperatures. Future work with longer panels and vehicle-vintage information could explicitly track whether newer BEV cohorts exhibit weaker temperature sensitivity, and whether social perceptions adjust at a similar pace.

Methods

Study Area and Time Period

This study utilizes ZIP code-level data from 12 US states over a three-year period (2021-2023). Public ZIP code-level BEV data are currently available for only 13 states, and of these, only a subset provides at least three years of historical records (see Figure S3 in Supplementary Information). Given the focus of this study on temperature effects, we selected states based on the breadth of climate conditions rather than length of data availability. The resulting panel includes the following states: California (CA), Colorado (CO), Connecticut (CT), Illinois (IL), Maine (ME), Minnesota (MN), New Jersey (NJ), New York (NY), North Carolina (NC), Oregon (OR), Texas (TX), and Vermont (VT). This sample spans all major Köppen climate classification zones found across the contiguous US[45], namely dry (BSk, BWh), temperate (Csa, Csb, Cfa, Cfb, Cwa), and continental (Dfa, Dfb, Dfc, Dsa, Dsb, Dsc, Dwb). Tropical classifications (Af and Aw), which in the conterminous US are largely confined to southern Florida, are excluded due to the absence of ZIP code-level data for this state. Nonetheless, these tropical zones account for just 5.9% of North America's land area[45], and their omission is unlikely to materially affect the climatic representativeness or generalizability of the findings within the continental US context. Overall, the broad climatic coverage of our panel dataset allows for a fine-grained geographic and climatic analysis that would not be possible using coarser, state-level data. Indeed, individual states often encompass multiple climate zones, potentially masking local variability.

Dependent Variable

The dependent variable in this study is BEV penetration, defined as the percentage of BEVs registered in a given ZIP code:

$$\text{BEV Penetration} = \frac{\text{BEV Population}}{\text{Total Vehicle Population}} * 100 \quad (1)$$

For most states in our sample (CO, CT, ME, MN, NJ, NY, NC, TX, VT), BEV population data was downloaded from Atlas EV Hub[46], while total vehicle population data was obtained from the US Census Bureau[47] American Community Survey 5-year estimates, as Atlas EV Hub does not provide total vehicle counts. For CA, IL, and OR, instead, BEV data were downloaded directly from governmental sources: the California Energy Commission[48] (CEC), the Illinois Secretary of State[49] (ILSOS), and the Oregon Department of Energy[50] (OR DOE), respectively. To account for differences in data sources and collection methods, ZIP code-level data were aggregated to the state level and compared with the BEV counts reported by the Alternative Fuels Data Center[51] (AFDC) of the US DOE and, when available, other state governmental sources, namely the Department of Environmental Protection (DEP)[52,53], the Public Utilities Commission (PUC)[54], or the Dallas-Fort Worth Clean Cities[55] (DFWCC). The close agreement across sources supports the validity of the dataset for analysis (see Fig. 2).

Explanatory Variables

The core explanatory variables are statistical descriptors of air temperature. These descriptors were derived in several steps following the approach of Cervini et al.[39]. First, we collected the geographic coordinates of all weather stations located within the 12 states of interest via the National Oceanic and Atmospheric Administration (NOAA)[56] Climate Data Online Web Services API. These stations provided daily minimum (T_{MIN}) and maximum (T_{MAX}) temperature data for the period 2021-2023. Second, we assigned each ZIP code the weather station closest to its centroid using a nearest neighbor approach, allowing for the construction of a ZIP code-level temperature dataset (see Fig. 3). From these data, annual distributions of T_{MIN} and T_{MAX} were computed for each ZIP code. A total of 43 temperature-derived variables were then calculated, including summary statistics such as minimum, maximum, mean, median, standard deviation, IQR, and 5th-95th percentiles, for both T_{MIN} and T_{MAX}.

We evaluated the correlation between each variable and BEV penetration (see Figure S4 in Supplementary Information). The variables that had the highest correlation were those related to distribution spread and low extremes. Based on this analysis, we retained $\overline{T}_{iqr}$ as our primary measure of variability, calculated as the IQR of daily mean temperatures within each year. Compared to standard deviation, IQR is less sensitive to outliers, providing a more robust measure of dispersion. Additionally, unlike metrics derived solely from T_{MIN} or T_{MAX}, $\overline{T}_{iqr}$ incorporates both daily minimum and maximum temperatures, offering a more comprehensive characterization of the ambient temperature range. We also included $T_{MIN<5}$, defined as the number of days in a year when the daily minimum temperature fell below 5°C, based on evidence by Walsh et al.[3], which shows that BEV driving range declines sharply when ambient temperatures drop below this threshold. $T_{MIN<5}$ was only moderately correlated with $\overline{T}_{iqr}$, allowing both to be retained without introducing multicollinearity. By contrast, several explicit "hot" indicators that we constructed (e.g., counts of days above 35°C) were highly collinear with $\overline{T}_{iqr}$ and $T_{MIN<5}$ and lost statistical insignificance once they were included in the model, adding little explanatory power while inflating multicollinearity.

Control Variables

Control variables were selected based on established determinants of BEV penetration identified in previous literature. These include sociodemographic descriptors, as well as charging infrastructure indicators. Sociodemographic descriptors were obtained through the US Census Bureau's API service, while charging infrastructure indicators were derived using the National Renewable Energy Laboratory (NREL)[57] API, which queries the database of the AFDC[58] and provides geolocated records of all public charging stations in the US from 2010 to the present. Following the method of Cervini et al.[39], we calculated the density of DCFC and Level 2 charging stations within each ZIP code, as well as the proximity to the nearest charging station, computed as the inverse of the distance between each ZIP code's population-weighted centroid and the nearest public charging station (see Fig. 4). The population weighted centroid data was collected from the US Department of Housing and Urban Development[59]. Following established approaches in the literature[60], we lag charging station densities by one year so that infrastructure stocks temporally precede the BEV outcome and reduce contemporaneous simultaneity between deployment and adoption. Because these lagged stock variables still reflect the cumulative history of prior build-out, some residual endogeneity may remain, and the corresponding coefficients should therefore be interpreted as conditional associations rather than fully causal effects. Identifying a causal effect of charging deployment on BEV penetration would require additional instruments, which are beyond the scope of this study.

Table 3 summarizes all variables included in the analysis, while Table S4 in Supplementary Information summarizes their descriptive statistics.

Model

To assess the relationship between ambient temperature and BEV penetration, we structured the dataset as a balanced panel at the ZIP code level spanning 2021 to 2023. ZIP codes with incomplete coverage across all years were excluded to ensure temporal and spatial consistency. Given the high spatial resolution and the likelihood of interdependence among neighboring units, we tested for spatial dependence using the Robust Lagrange Multiplier (RLM) framework adapted for panel data, following the procedure recommended by Millo[61]. This approach requires time- and cross-sectionally demeaning the data before applying the tests to remove individual and time effects which can significantly affect their empirical properties. Specifically, we employed: (1) the RLM lag test to assess spatial autocorrelation in the dependent variable, and (2) the RLM error test to detect spatial autocorrelation in the residuals. Both tests were implemented using the `panel_rLMlag` and `panel_rLMerror` functions from the `spreg` Python package by Anselin, Luc[62]. The results provided strong evidence of both forms of spatial dependence (RLM lag = 234.37, $p < 0.01$;

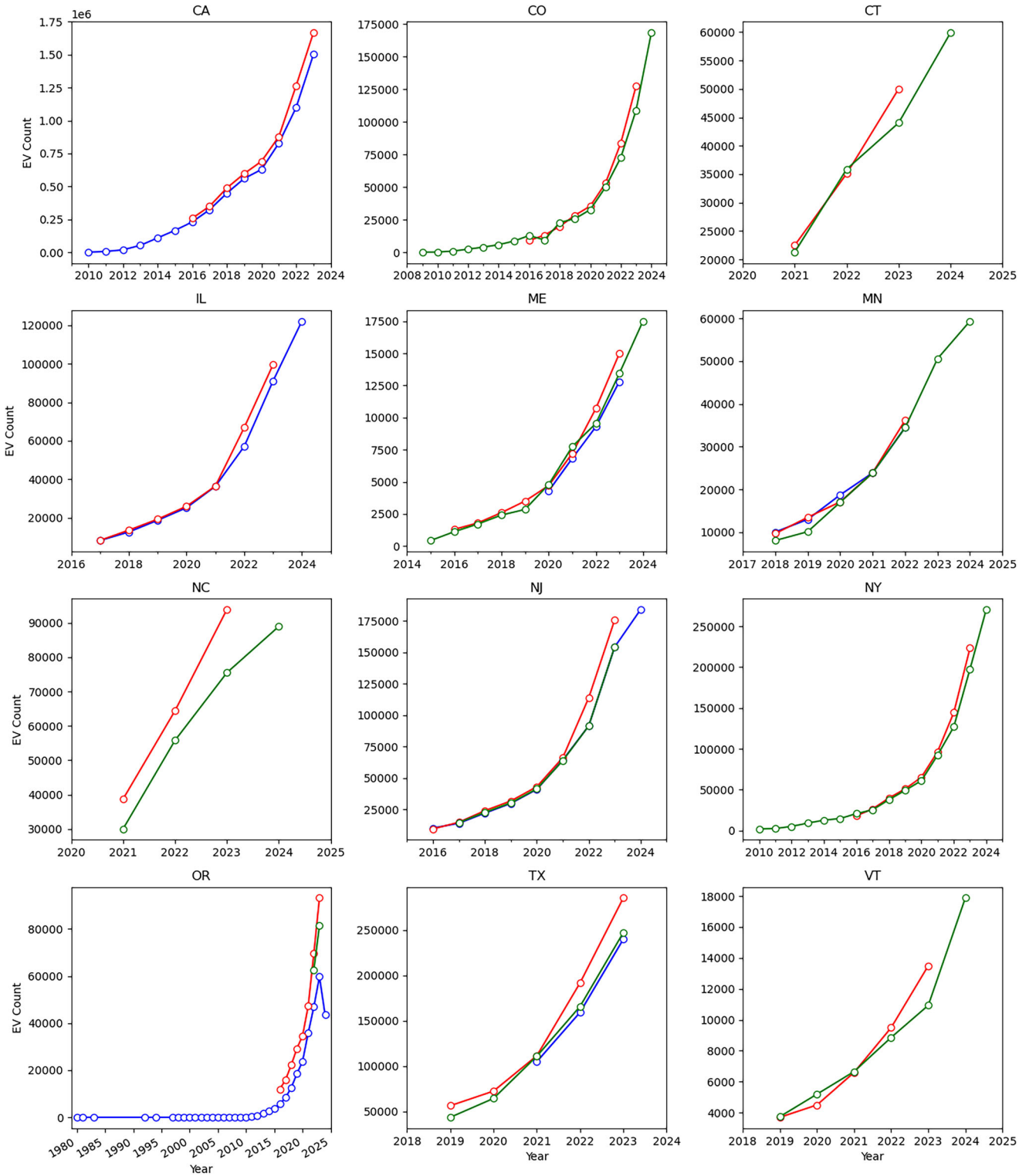

Fig. 2 | Validation of BEV registration data. Each panel compares our ZIP code-aggregated BEV counts with external benchmarks for each state, showing close agreement across data sources. In each panel, the red line denotes the US DOE benchmark series, the blue line denotes a state-government series when available (CEC for CA; ILSOS for IL; ME DEP for ME; MN PUC for MN, NJ DEP for NJ; OR DOE for OR; DFWCC for TX), while the green line denotes totals derived from Atlas EV Hub where used.

RLM error = 117.85, $p < 0.01$), motivating the use of a Spatial Autoregressive Model with Autoregressive Disturbances (SARAR), defined as:

$$y = \rho W y + X\beta + u, \tag{2}$$

$$u = \lambda W u + \varepsilon \tag{3}$$

Here, y denotes BEV penetration; W is a row-standardized spatial weights matrix constructed using Queen contiguity, and X is a matrix of

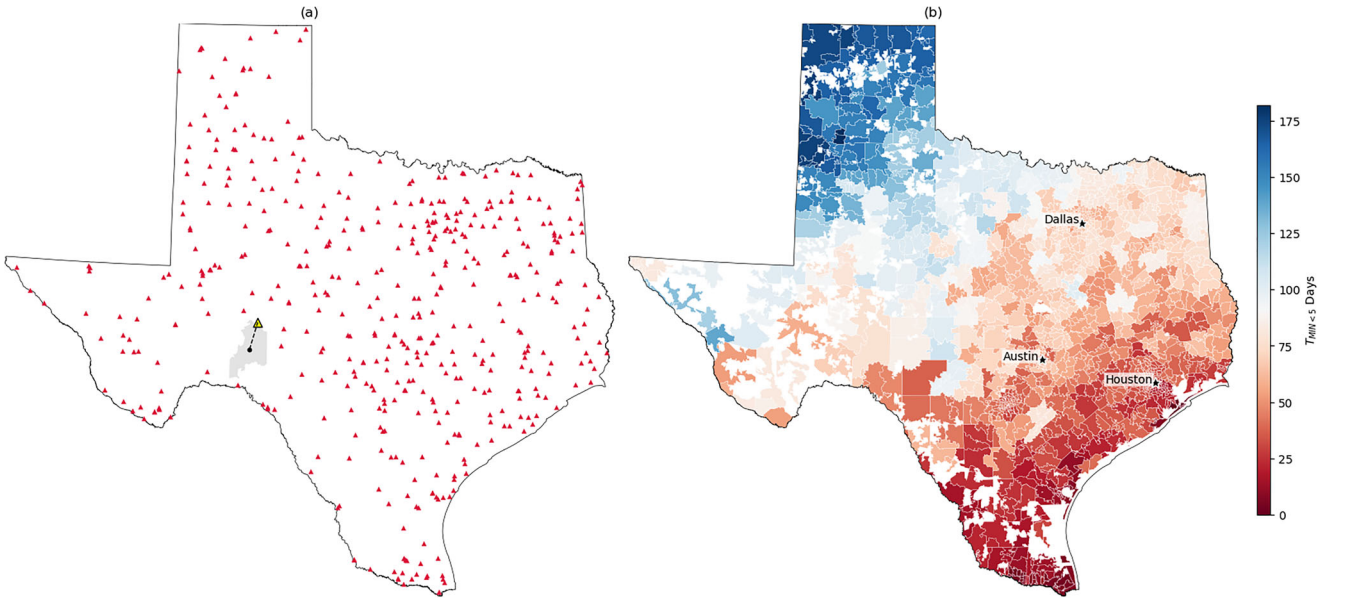

Fig. 3 | Construction of ZIP code level temperature variables: TX example. **(a)** Illustration of the nearest-neighbor assignment approach: the ZIP code centroid (black dot) of ZIP 76943 (gray polygon) is linked to its closest weather station (yellow triangle), selected from the network of NOAA weather stations (red triangles) across the state. **(b)** Resulting spatial distribution of one temperature-derived variable, $T_{MIN<5}$, aggregated to the ZIP code level, with darker blue indicating more cold days and darker red indicating fewer cold days. Major cities are labeled for orientation.

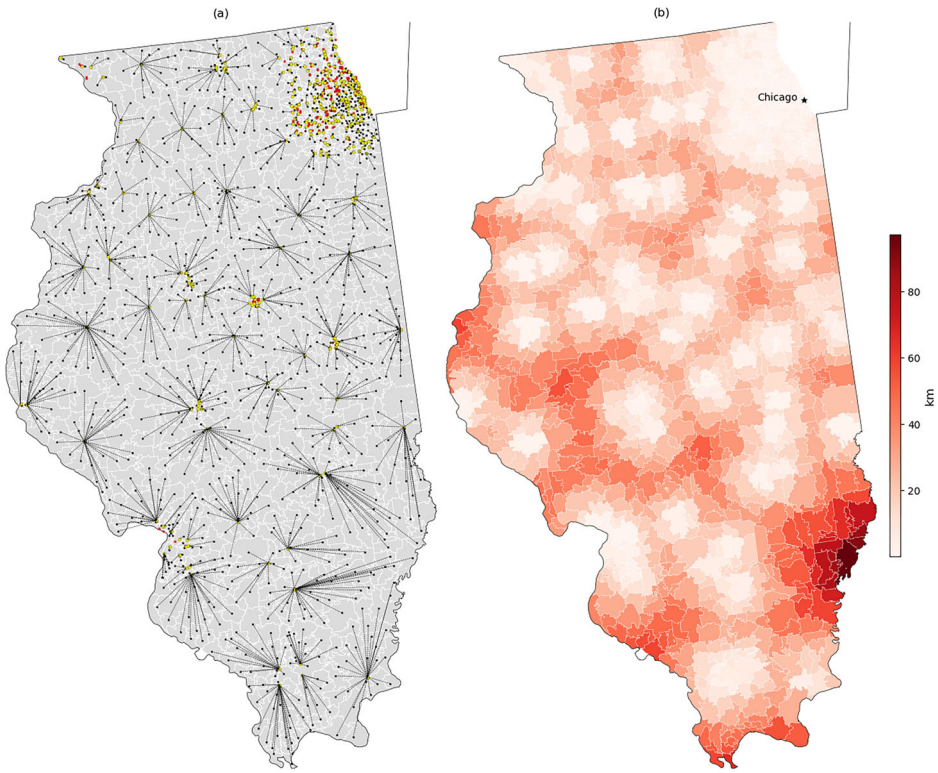

Fig. 4 | Derivation of ZIP code level charging metrics: IL 2021 example. (**a**) Computation of the distance to the nearest charging station for each ZIP code. ZIP codes are shown as light-gray polygons. Black dots mark population-weighted ZIP code centroids. Red circles denote public charging stations. For each ZIP code, the nearest charging station is highlighted with a yellow circle, and the dashed black segment shows the centroid-to-station connection used to compute distance. (**b**) Resulting ZIP code level dataset, showing the distance to the nearest public charging station, with darker red indicating larger distances. The Chicago location marker is included for orientation.

covariates each multiplied by its own coefficient β. The parameter ρ captures spatial lag dependence in the outcome variable, while λ captures spatial autocorrelation in the unobserved component u, which itself follows a spatial autoregressive structure. ε is an i.i.d. error term.

To determine the appropriate panel specification, we tested for correlation between the regressors and unobserved unit-specific effects using the Hausman test. Both FE and random effects (RE) versions of the model were estimated with full inclusion of spatial terms, in accordance with recent methodological guidance by Millo[61]. The Hausman test, implemented via the `panel_Hausman` function from the `spreg` package, returned a test statistic of 1043.81 ($p < 0.01$), rejecting the null hypothesis of orthogonality and supporting the use of a FE specification.

To flexibly capture the empirically observed association between annual temperature variability and BEV penetration, we replace the single $\overline{T}_{iqr}$ regressor with a piecewise-linear spline. Concretely, we generate three

Table 3 | Summary of variables used in this analysis

Variable	Definition	Unit
Dependent variable		
BEV Penetration	Share of BEVs in the total vehicle population	%
Explanatory variables		
$\overline{T}_{iqr}$	Daily mean temperature inter-quartile range in a year	°C
$T_{MIN<5}$	Number of days in a year minimum temperature falls below 5°C	days
Control variables		
Station Proximity	Proximity to the nearest charging station; higher values indicate closer proximity	1/km
Level 2 Stations	Lagged density of Level 2 charging stations	stations/km^2
DCFC Stations	Lagged density of DC fast charging stations	stations/km^2
Housing Density	Density of housing units	1,000 units/km^2
Multivehicle HH	Households with more than one vehicle	%
Solar Energy HH	Households using solar energy for heating	%
Public Transit	Population commuting via public transit	%
Commute Time	Mean travel time to work	10 minutes
Income	Median household income	$10,000
Education	Population with a graduate degree	%

basis functions $B_1(\overline{T}_{iqr})$, $B_2(\overline{T}_{iqr})$, $B_3(\overline{T}_{iqr})$ via a first-degree B-spline with internal knots positioned at the 15th and 85th percentiles of the empirical $\overline{T}_{iqr}$ distribution (11.4°C and 18.4°C). This yields three segments-low, moderate, and high variability-within which the marginal effect of a 1°C increase in $\overline{T}_{iqr}$ is allowed to differ, yet the curve remains continuous at each knot.

Our final model is a two-way FE SARAR, expressed as:

$$y_{zst} = \rho W y_{zst} + \beta X_{zst} + \alpha_s * \gamma_t + u_{zst} \quad (4)$$

$$u_{zst} = \lambda W u_{zst} + \varepsilon_{zst} \quad (5)$$

In this formulation, y_{zst} is BEV penetration in ZIP code z, state s, and year t; $\rho W y_{zst}$ is the spatial lag; βX_{zst} collects all of our explanatory and control variables, including the piecewise-linear spline on $\overline{T}_{iqr}$, with coefficients β; α_s and γ_t are state and year FE, respectively, controlling for unobserved, time-invariant heterogeneity across states and common shocks across years. Finally, the composite disturbance u_{zst} follows its own spatial-error process, where λ captures residual spatial autocorrelation and ε_{zst} is an i.i.d. error.

Rather than including additive state and year FE (i.e., $\alpha_s + \gamma_t$), we specify our model with fully interacted state-by-year FE (i.e., $\alpha_s{}^*\gamma_t$). This decision reflects the possibility that the influence of unobserved state-level factors on BEV penetration may evolve over time in non-parallel, non-additive ways. For instance, states may implement new incentives, update regulatory frameworks, or experience infrastructure developments at different points in time, leading to dynamic, state-specific shifts in BEV penetration that would not be adequately captured by separate state and year effects. By using the full interaction, we flexibly control for all time-varying unobservables at the state level, absorbing any unobserved shocks specific to a state in a given year, in addition to common unobserved macroeconomic shocks that uniformly affect all states. Overall, this specification addresses two central features of the data: (1) unobserved heterogeneity across space and time, which, if uncontrolled, may bias estimates; and (2) spatial autocorrelation arising from policy diffusion, peer influence, or regional market dynamics, which introduces dependencies among geographically proximate ZIP codes.

For comparison, we also estimate a two-way FE OLS model without spatial terms:

$$y_{zst} = \beta X_{zst} + \alpha_s * \gamma_t + \varepsilon_{zst} \quad (6)$$

This non-spatial model is estimated using the `PanelOLS` function from the `linearmodels` package by Kevin Sheppard[63], and serves to benchmark the incremental explanatory power of spatial dependence.

Spillover Effects

In spatial models, the coefficient ρ introduces feedback effects: a change in an explanatory variable in one unit may affect outcomes in neighboring units (indirect or spillover effects), as well as the unit itself (direct effects). To quantify these impacts, we follow LeSage and Pace[64], decomposing the total effect of each covariate into direct and indirect components using the spatial multiplier matrix $\mathbf{S} = (\mathbf{I} - \rho\mathbf{W})^{-1}$. For each covariate k in the vector of regressors X, the average effects are computed as:

$$\text{Direct}_k = \frac{1}{n}\text{tr}(\mathbf{S}) \cdot \beta_k \quad (7)$$

$$\text{Total}_k = \frac{1}{n}\mathbf{1}^\top \mathbf{S}\mathbf{1} \cdot \beta_k \quad (8)$$

$$\text{Indirect}_k = \text{Total}_k - \text{Direct}_k \quad (9)$$

where n is the number of ZIP codes, $tr(\cdot)$ denotes the matrix trace, and 1 is a vector of ones. This decomposition enables interpretation of both localized and spatially mediated impacts of explanatory variables on BEV penetration.

Data availability

All datasets analyzed in this study are publicly available from the original sources listed below. Vehicle registration data were obtained from publicly accessible databases and state agencies, including the US Census Bureau (https://data.census.gov/table), Atlas Public Policy (https://www.atlasevhub.com/), California Energy Commission (https://www.energy.ca.gov/files/zev-and-infrastructure-stats-data), Illinois Secretary of State (https://www.ilsos.gov/departments/vehicles/statistics/electric/home.html), Oregon Department of Energy (https://www.oregon.gov/energy/Data-and-Reports/Pages/Oregon-Electric-Vehicle-Dashboard.aspx), Alternative Fuels Data Center (https://afdc.energy.gov/vehicle-registration), Maine Department of Environmental Protection (https://www.maine.gov/dep/air/mobile/vehicle-data.html), New Jersey Department of Environmental Protection (https://dep.nj.gov/drivegreen/nj-ev-data/), Minnesota Public Utilities Commission (https://mn.gov/puc/activities/economic-analysis/electric-vehicles/), and Dallas-Fort Worth Clean Cities (https://www.dfwcleancities.org/evsintexas). Weather station data were obtained from the NOAA Web Services API (https://www.ncdc.noaa.gov/cdo-web/webservices/v2). Data on charging infrastructure were obtained from the Alternative Fuels Data Center (https://afdc.energy.gov/fuels/electricity-locations). ZIP Code Tabulation Area boundary shapefiles were obtained from the US Census Bureau TIGER/line repositories (https://www.census.gov/geographies/mapping-files/time-series/geo/tiger-line-file.html), and population weighted ZIP code centroids were obtained from the US Department of Housing and Urban Development (https://hudgis-hud.opendata.arcgis.com/datasets/d032efff520b4bf0aa620a54a477c70e/explore).

Received: 11 June 2025; Accepted: 21 April 2026;
Published online: 03 June 2026

References

1. Argonne National Laboratory. Light duty electric drive vehicles monthly sales updates. https://www.anl.gov/esia/light-duty-electric-drive-vehicles-monthly-sales-updates (2025). Accessed June 9, 2025.
2. U.S. Department of Energy. Alternative fuels data center: Data (2024). https://afdc.energy.gov/data/10962. Accessed June 9, 2025.
3. Walsh, P. et al. Impact of cold ambient temperature and extreme conditions on electric vehicles. Program Record, Vehicle Technologies Office (2024). Approved by Sarah Ollila and Austin Brown (DOE) on 09/23/2024.
4. Yuksel, T. & Michalek, J. J. Effects of regional temperature on electric vehicle efficiency, range, and emissions in the United States. *Environ. Sci. Technol.* **49**, 3974–3980 (2015).
5. Koncar, I. & Bayram, I. S. A probabilistic methodology to quantify the impacts of cold weather on electric vehicle demand: A case study in the U.K. *IEEE Access* **9**, 88205–88216 (2021).
6. Hao, X., Wang, H., Lin, Z. & Ouyang, M. Seasonal effects on electric vehicle energy consumption and driving range: A case study on personal, taxi, and ridesharing vehicles. *J. Clean. Prod.* **249**, 119403 (2020).
7. Suarez-Bertoa, R. et al. Effect of low ambient temperature on emissions and electric range of plug-in hybrid electric vehicles. *ACS Omega* **4**, 3159–3168 (2019).
8. Zhao, C. et al. Research on electric vehicle range under cold condition. *Adv. Mech. Eng.* **14**, 16878132221087083 (2022).
9. Fetene, G. M., Kaplan, S., Mabit, S. L., Jensen, A. F. & Prato, C. G. Harnessing big data for estimating the energy consumption and driving range of electric vehicles. *Transportation Res. Part D: Transp. Environ.* **54**, 1–11 (2017).
10. Zou, Y., Wei, S., Sun, F., Hu, X. & Shiao, Y. Large-scale deployment of electric taxis in Beijing: A real-world analysis. *Energy* **100**, 25–39 (2016).
11. Mahmoudzadeh Andwari, A., Pesiridis, A., Rajoo, S., Martinez-Botas, R. & Esfahanian, V. A review of battery electric vehicle technology and readiness levels. *Renew. Sustain. Energy Rev.* **78**, 414–430 (2017).
12. Lindgren, J. & Lund, P. D. Effect of extreme temperatures on battery charging and performance of electric vehicles. *J. Power Sources* **328**, 37–45 (2016).
13. Senol, M., Bayram, I. S., Naderi, Y. & Galloway, S. Electric vehicles under low temperatures: A review on battery performance, charging needs, and power grid impacts. *IEEE Access* **11**, 39879–39912 (2023).
14. Kambly, K. R. & Bradley, T. H. Estimating the HVAC energy consumption of plug-in electric vehicles. *J. Power Sources* **259**, 117–124 (2014).
15. Wu, H., Chen, J., Vaishnav, P., Sun, M. & Craig, M. T. Technological improvements in EV batteries offset climate-induced durability challenges. *Nat. Clim. Change* **16**, 460–467 (2026).
16. Sun, P., Bisschop, R., Niu, H. & Huang, X. A review of battery fires in electric vehicles. *Fire Technol.* **56**, 1361–1410 (2020).
17. Cui, Q. et al. Weather effects on highway travel volume: Electric vs. fuel vehicles. *Transportation Res. Part D: Transp. Environ.* **145**, 104805 (2025).
18. Gu, J., Liao, Q. & Zhang, K. M. Assessing the cold weather impact on battery electric transit buses. *Transportation Res. Part D: Transp. Environ.* **145**, 104809 (2025).
19. Alotaibi, S., Omer, S., Aljarallah, S. & Su, Y. Potential implementation of EVs - features, challenges and user perspective. In *2021 IEEE Green Energy and Smart Systems Conference (IGESSC)*, 1-10 (2021).
20. She, Z.-Y., Sun, Q., Ma, J.-J. & Xie, B.-C. What are the barriers to widespread adoption of battery electric vehicles? A survey of public perception in Tianjin, China. *Transp. Policy* **56**, 29–40 (2017).
21. Zhang, X., Bai, X. & Zhong, H. Electric vehicle adoption in license plate-controlled big cities: Evidence from Beijing. *J. Clean. Prod.* **202**, 191–196 (2018).
22. Almeida Neves, S., Cardoso Marques, A. & Alberto Fuinhas, J. Technological progress and other factors behind the adoption of electric vehicles: Empirical evidence for EU countries. *Res. Transportation Econ.* **74**, 28–39 (2019).
23. Singh, V., Singh, V. & Vaibhav, S. A review and simple meta-analysis of factors influencing adoption of electric vehicles. *Transportation Res. Part D: Transp. Environ.* **86**, 102436 (2020).
24. Alotaibi, S., Omer, S. & Su, Y. Identification of potential barriers to electric vehicle adoption in oil-producing nations-the case of Saudi Arabia. *Electricity* **3**, 365–395 (2022).
25. Jia, W. & Chen, T. D. Are individuals' stated preferences for electric vehicles (evs) consistent with real-world EV ownership patterns? *Transportation Res. Part D: Transp. Environ.* **93**, 102728 (2021).
26. Kamis, A. & Abraham, P. S. Predictive models of electric vehicle adoption in the United States: Charging ahead with renewable energy. *Transportation Res. Interdiscip. Perspect.* **24**, 101041 (2024).
27. Lee, J. H., Hardman, S. J. & Tal, G. Who is buying electric vehicles in California? Characterising early adopter heterogeneity and forecasting market diffusion. *Energy Res. Soc. Sci.* **55**, 218–226 (2019).
28. Rotaris, L., Giansoldati, M. & Scorrano, M. The slow uptake of electric cars in Italy and Slovenia. Evidence from a stated-preference survey and the role of knowledge and environmental awareness. *Transportation Res. Part A: Policy Pract.* **144**, 1–18 (2021).
29. Sinton, J., Cervini, G., Gkritza, K., Labi, S. & Song, Z. Examining electric vehicle adoption at the postal code level in US states. *Transportation Res. Part D: Transp. Environ.* **127**, 104068 (2024).
30. Yang, A., Liu, C., Yang, D. & Lu, C. Electric vehicle adoption in a mature market: A case study of Norway. *J. Transp. Geogr.* **106**, 103489 (2023).
31. Burra, L. T., Al-Khasawneh, M. B. & Cirillo, C. Impact of charging infrastructure on electric vehicle adoption: A synthetic population approach. *Travel Behav. Soc.* **37**, 100834 (2024).
32. Hardman, S., Chandan, A., Tal, G. & Turrentine, T. The effectiveness of financial purchase incentives for battery electric vehicles–a review of the evidence. *Renew. Sustain. Energy Rev.* **80**, 1100–1111 (2017).
33. Coffman, M., Bernstein, P. & Wee, S. Electric vehicles revisited: a review of factors that affect adoption. *Transp. Rev.* **37**, 79–93 (2017).
34. Li, X., Zhao, X., Xue, D. & Tian, Q. Impact of regional temperature on the adoption of electric vehicles: An empirical study based on 20 provinces in China. *Environ. Sci. Pollut. Res.* **30**, 11443–11457 (2023).
35. Gao, J., Zhang, N. & Zhang, T. Cold waves and electric vehicle adoption: Evidence from chinese cities. *Transportation Res. Part D: Transp. Environ.* **143**, 104748 (2025).
36. Vergis, S. & Chen, B. Comparison of plug-in electric vehicle adoption in the United States: A state by state approach. *Res. Transportation Econ.* **52**, 56–64 (2015).
37. Lee, A., Yong, J. & Nilsson, I. An examination of the effect of external factors on zero-emission vehicle adoption in the United States. *Travel Behav. Soc.* **38**, 100904 (2025).
38. Jelinski, D. E. & Wu, J. The modifiable areal unit problem and implications for landscape ecology. *Landsc. Ecol.* **11**, 129–140 (1996).
39. Cervini, G., Jung, J. & Gkritza, K. Temperature and electric vehicle adoption: A zip code-level analysis in the US. *Transportation Res. Part D: Transp. Environ.* **136**, 104435 (2024).
40. Yuan, Q. et al. Investigation on range anxiety and safety buffer of battery electric vehicle drivers. *J. Adv. Transportation* **2018**, 8301209 (2018).
41. Xia, L., Chen, C., Ren, H. & Kang, Z. Analysis of range anxiety using NEV monitoring big data. In *2022 Asia Conference on Algorithms, Computing and Machine Learning (CACML)*, 145-149 (IEEE, 2022).
42. Hardaway, K., Genc, U., Cai, H. & Nateghi, R. Electric vehicle adoption and planning: The increasing importance of the built environment. *J. Transp. Geogr.* **123**, 104115 (2025).

43. Zhang, B., Niu, N., Li, H., Wang, Z. & He, W. Could fast battery charging effectively mitigate range anxiety in electric vehicle usage? Evidence from large-scale data on travel and charging in Beijing. *Transportation Res. Part D: Transp. Environ.* **95**, 102840 (2021).
44. Trinko, D. et al. Economic feasibility of in-motion wireless power transfer in a high-density traffic corridor. *eTransportation* **11**, 100154 (2022).
45. Peel, M. C., Finlayson, B. L. & McMahon, T. A. Updated world map of the Köppen–Geiger climate classification. *Hydrol. Earth Syst. Sci.* **11**, 1633–1644 (2007).
46. Atlas Public Policy. Atlas EV hub (2024). https://www.atlasevhub.com. Accessed June 9, 2025.
47. US Census Bureau. Data tables (2024). https://data.census.gov/table. Accessed June 9, 2025.
48. California Energy Commission. ZEV and infrastructure stats data (2024). https://www.energy.ca.gov/files/zev-and-infrastructure-stats-data. Accessed June 9, 2025.
49. Illinois Secretary of State. Electric vehicle counts by county (2024). https://www.ilsos.gov/departments/vehicles/statistics/electric/home.html. Accessed June 9, 2025.
50. Oregon Department of Energy. Data and reports (2024). https://www.oregon.gov/energy/Data-and-Reports/Pages/default.aspx. Accessed June 9, 2025.
51. Alternative Fuels Data Center. Vehicle registration data. https://afdc.energy.gov/vehicle-registration (2024). Accessed June 9, 2025.
52. Maine Department of Environmental Protection. Vehicle data and reports (2024). https://www.maine.gov/dep/air/mobile/vehicle-data.html. Accessed June 9, 2025.
53. New Jersey Department of Environmental Protection. New Jersey EV data (2024). https://dep.nj.gov/drivegreen/nj-ev-data/. Accessed June 9, 2025.
54. Minnesota Public Utilities Commission. Electric vehicles in Minnesota (2024). https://mn.gov/puc/activities/economic-analysis/electric-vehicles/. Accessed June 9, 2025.
55. Dallas-Fort Worth Clean Cities. EVs in texas (2024). https://www.dfwcleancities.org/evsintexas. Accessed June 9, 2025.
56. National Oceanic and Atmospheric Administration (NOAA). Web services api (version 2) documentation (n.d.). https://www.ncdc.noaa.gov/cdo-web/webservices/v2. Accessed June 9, 2025.
57. National Renewable Energy Laboratory (NREL). Alternative fuel stations api (version 1) documentation (n.d.). https://developer.nrel.gov/docs/transportation/alt-fuel-stations-v1/. Accessed June 9, 2025.
58. Alternative Fuels Data Center. Alternative fuels data center: Electric vehicle charging station locations (2024). https://afdc.energy.gov/fuels/electricity-locations. Accessed June 9, 2025.
59. US Department of Housing and Urban Development. Zip code population weighted centroids. HUD (2024). https://hudgis-hud.opendata.arcgis.com/datasets/d032efff520b4bf0aa620a54a477c70e/explore. Accessed June 9, 2025.
60. Narassimhan, E. & Johnson, C. The role of demand-side incentives and charging infrastructure on plug-in electric vehicle adoption: Analysis of US states. *Environ. Res. Lett.* **13**, 074032 (2018).
61. Millo, G. Empirical behaviour of Anselin et al.'s locally robust lm tests for spatial dependence in a panel data setting. *Regional Sci. Urban Econ.* **112**, 104106 (2025).
62. Anselin, L. *spreg*. https://pypi.org/project/spreg/ (2025). Accessed June 9, 2025.
63. Sheppard, K. *linearmodels*. https://pypi.org/project/linearmodels/ (2024). Accessed June 9, 2025.
64. LeSage, J. & Pace, R. K.*Introduction to Spatial Econometrics* (Chapman and Hall/CRC, New York, 2009).

Acknowledgements

This study was supported by the Advancing Self-Sufficiency through Powered Infrastructure for Roadway Electrification (ASPIRE) Engineering Research Center funded by the National Science Foundation under Grant No. 1941524. The authors gratefully acknowledge Felix Michael Stimets for his assistance with BEV data collection and the literature review.

Author contributions

G.C. led the conceptualization, investigation, data curation, formal analysis, code development, figure preparation, and drafting of the manuscript. G.C., L.T.B., J.J., and K.G. jointly developed the methodology, contributed to conceptual development, and performed validation. J.J. and K.G. provided supervision and project administration. K.G. acquired funding for the project. All authors reviewed and edited the manuscript.

Competing interests

The authors declare no competing interests.

Additional information

Supplementary information The online version contains supplementary material available at https://doi.org/10.1038/s44333-026-00109-0.

Correspondence and requests for materials should be addressed to Gaia Cervini.